Biosensors and Bioelectronics 239 (2023) 115609



Contents lists available at ScienceDirect

Biosensors and Bioelectronics

journal homepage: www.elsevier.com/locate/bios



# A universal all-in-one RPA-Cas12a strategy with de novo autodesigner and its application in on-site ultrasensitive detection of DNA and RNA viruses

Cailing Lin [a,1], Feng Chen [a,1], Dongchao Huang [a,1], Wenyan Li [a], Changsheng He [a,h], Yingjun Tang [g], Xueping Li [c], Can Liu [d,e], Liya Han [a], Yunpeng Yang [a], Yongchong Zhu [a], Ruikang Chen [a], Yuanju Shi [c], Chenglai Xia [d,e], Zhibin Yan [f], Hongli Du [a], Lizhen Huang [a,b,*]

[a] School of Biology and Biological Engineering, South China University of Technology, Guangzhou, 510006, China
[b] Fangrui Institute of Innovative Drugs, South China University of Technology, Guangzhou, 510006, China
[c] Guangzhou Yoyoung Bio-tech Company, Guangzhou, 510300, China
[d] Affiliated Foshan Maternity and Child Healthcare Hospital, Southern Medical University, Foshan, 528000, China
[e] School of Pharmaceutical Sciences, Southern Medical University, Guangzhou, 515150, China
[f] Guangdong Provincial Key Laboratory of Optical Information Materials and Technology & Institute of Electronic Paper Displays, South China Academy of Advanced Optoelectronics, South China Normal University, Guangzhou, 510006, PR China
[g] WENS Foodstuff Group Co., Ltd., Yunfu, 527400, China
[h] Experimental Animal Center, Nanfang Hospital, Southern Medical University, Guangzhou, 510515, China

ARTICLE INFO

*Keywords:*
One-pot
CRISPR/Cas12
Virus detection
Portable device
Automation design

ABSTRACT

Revolutionary all-in-one RPA-CRISPR assays are rapidly becoming the most sought-after tools for point-of-care testing (POCT) due to their high sensitivity and ease of use. Despite the availability of one-pot methods for specific targets, the development of more efficient methods for new targets remains a significant challenge. In this study, we present a rapid and universal approach to establishing an all-in-one RPA-Cas12a method CORDSv2 based on rational balancing amplification and Cas12a cleavage, which achieves ultrasensitive detection of several targets, including SARS-CoV-2, ASFV, HPV16, and HPV18. CORDSv2 demonstrates a limit of detection (LOD) of 0.6 cp/μL and 100% sensitivity for SARS-CoV-2, comparable to qPCR. Combining with our portable device(hippo-CORDS), it has a visual detection LOD of 6 cp/μL and a sensitivity up to 100% for SARS-CoV-2 and 97% for Ct<35 ASFV samples, surpassing most one-pot visual methods. To simplify and accelerate the process for new targets, we also develop a de novo autodesigner by which the optimal couples of primers and crRNA can be selected rapidly. As a universal all-in-one RPA-CRISPR method for on-site testing, CORDSv2 becomes an attractive choice for rapid and accurate diagnosis in resource-limited settings.

## 1. Introduction

The RNA-guided CRISPR/Cas (Clustered Regularly Interspaced Short Palindromic Repeats/CRISPR-associated system) holds significant potential for next-generation point-of-care (POC) molecular diagnostics, as it enables single-base precision targeting and rapid, nonspecific nucleic acid cleavage at a single reaction temperature (Zhang et al., 2022). Numerous sensitive and specific detection platforms have been developed by combining CRISPR/Cas type V and type VI with isothermal amplification methods, such as SHERLOCK, DETECTR, HOLMES, CORDS, iSCAN, CDetection, and CARMEN (Ackerman et al., 2020; Ali et al., 2020; Bai et al., 2019; Broughton et al., 2020; Kellner et al., 2019; Li et al., 2018; Teng et al., 2019). These platforms can identify DNA and RNA viruses at aM sensitivity levels, rivaling qPCR. However, most CRISPR-based tests require two separate operational steps – isothermal amplification and CRISPR/Cas-based cleavage – which complicate the process and hinder widespread adoption. Combining isothermal amplification and CRISPR/Cas cleavage in a single tube is essential but challenging due to the potential reduction in amplification efficiency caused by Cas-mediated cleavage of newly synthesized amplicons (Ali et al., 2020; Nguyen et al., 2022).

Previous one-pot studies have attempted to address this issue by

* Corresponding author. School of Biology and Biological Engineering, South China University of Technology, Guangzhou, 510006, China.
*E-mail address:* huanglzh@scut.edu.cn (L. Huang).
[1] These authors contributed equally to this work: Cailing Lin, Feng Chen, Dongchao Huang.

https://doi.org/10.1016/j.bios.2023.115609
Received 12 June 2023; Received in revised form 23 July 2023; Accepted 16 August 2023
Available online 18 August 2023
0956-5663/© 2023 The Authors. Published by Elsevier B.V. This is an open access article under the CC BY-NC-ND license (http://creativecommons.org/licenses/by-nc-nd/4.0/).

separating CRISPR/Cas reagents from the amplification reaction initially, then combining them at the end of the amplification process (Kostyusheva et al., 2022). Other strategies included optically switching on crRNA after amplification, systematically optimizing the reaction system and using PAM-free or suboptimal crRNA (Aman et al., 2020; Chen et al., 2022; Hu et al., 2022; Malci et al., 2022). Several one-pot methods with ssDNA-targeted crRNA achieved highly sensitive detection by cleverly designing PAM-free crRNA near the amplification primers, including AOID-CRISPR, CODA, RADICA and 3D assay (Ding et al., 2020; Lee et al., 2021; Wu et al., 2021; Xia et al., 2023). The resulting single-strand cleavage by PAM-free crRNA was demonstrated to not affect the amplification process, making both reactions could occur simultaneously in a single tube. In addition to canonical PAM, sPAMC (suboptimal PAM of Cas12a-based test) also exhibited faster reaction kinetics and higher sensitivity in a one-pot reaction (Lu et al., 2022). However, these methods have their limitations, such as complicated sequential operations, location restrictions and totally different designing principles for crRNA and primers, unclear optimization mechanisms and unfeasibility for more new targets.

To overcome these challenges, we proposed an improved all-in-one Cas12a-based rapid detection system called CORDSv2, building on our earlier CORDSv1 (Bai et al., 2019). We first examined the issues present in existing one-pot systems, including the optimal buffer environment compatibility for isothermal amplification and CRISPR/Cas12a reactions, the interaction of initial Cas12a cleavage with amplification, and probe stability. We then optimized the reaction buffer and probe to establish an effective one-pot system. Furthermore, we investigated strategies to achieve a balance between isothermal amplification and CRISPR/Cas12a reactions by analyzing the dynamics of various crRNAs and recombinase polymerase amplification (RPA) primers.

Our CORDSv2 platform enables a rational design of crRNA and primers that balances the relationship between amplification and Cas12 cleavage and improves the sensitivity of the one-pot system up to 0.6 cp/μL, comparable to traditional two-step methods and qPCR (Kostyusheva et al., 2022). To simplify and accelerate the process for new targets, a de novo autodesigner for CORDSv2 was also developed by which the optimal couples of primers and crRNA can be selected rapidly. The platform has been validated for multiple targets of different viruses. This approach demonstrates that a sensitive and accurate one-pot Cas12 assay can be achieved conveniently and rapidly, paving the way for broader applications of CRISPR/Cas-based POC testing.

## 2. Results

### 2.1. Obtaining ultrasensitive one-pot CORDSv2 by rational balancing amplification and Cas12a cleavage

The initial two-pot CORDSv1 has successfully identified viruses including ASFV, SARC-CoV-2, and its variants by fluorescence signal or colorimetric lateral-flow strip with two pots (Bai et al., 2019; He et al., 2022). With crRNA and RPA primers targeting SARS-CoV-2 N, the sensitivity of CORDSv1-SARS reached $10^{-17}$ M with fluorescent readout and $10^{-15}$ M with lateral flow readout (Figs. S2A and S2B). However, the detection sensitivity decreased significantly when integrating the RPA and Cas12a reactions into one tube according to the reported strategies (de Puig et al., 2021; Feng et al., 2021; Lee et al., 2020), even failing to identify $10^{-11}$ M DNA template (Fig. S1A). In order to develop one-tube CORDS rationally and reliably, we first attempted to find out the interplay between RPA and Cas12a reaction in one tube and then perform optimization accordingly.

Compared with the negative group by two-pot, the fluorescence signal of negative in one-pot was much higher and also increased obviously over time even without any active ribonucleoprotein (RNP) of Cas12a/crRNA (Fig. S1A). This indicated that the probe with 12 nt random sequence (5′-FAM-NNNNNNNNNNNN-BHQ1-3′) might not be stable in one-pot system, although it performed well in our previous two-pot system. To further discover the reason behind this, the ssDNA probe was added to the only RPA isothermal amplification mixture. After incubation at 37 °C for 30 min, fluorescence raised accordingly with the increase of RPA enzyme concentration, suggesting that ssDNA probe might be cleaved because of the intrinsic exonuclease activity of DNA polymerases within RPA mix (Fig. S1B) (Li et al., 2020; Zyrina and Antipova, 2021). The nonspecific cleavage of probe would seriously interfere with detection readout relying on specific cleavage by activated RNP. To solve this problem, we designed two additional DNA probes 5 nt probe FQ2 and G-triplex probe FQ3, by adjusting the length and secondary structure based on the trans-cleavage feature of Cas12a. The comparison of the three probes indicated that probe FQ2 (5′-FAM-TTATT-BHQ1-3′) was much less consumed by RPA than the other two probes, showing the best stability (Fig. 1A). And FQ2 was also more likely trans-cleaved by CRISPR/Cas12a (Fig. 1B). Therefore, FQ2 was considered as the better choice for one-pot reaction.

To further examine the influence of Cas12a on RPA in one-pot mixture, the RPA product was isolated and purified from the mixture after incubation at 37 °C for 30 min. There was no accumulation of specific amplicons in the system with activated RNP, but obviously accumulation with inactive RNP (Fig. S1C). This showed that active Cas12a might inhibit RPA amplification in one tube by consuming the initial template excessively. To weaken the consumption of the amplification substrate by Cas12a, we attempted to optimize the reaction buffer by comparing the effects of three buffers from different RPA kits on the activity of Cas12a. The activity of Cas12a with AMP Future buffer was the lowest, whereas the highest fluorescence and most favorable for one-pot detection (Fig. 1C and D). Further optimization including the component concentration and reaction temperature was also carried out to improve the one-pot performance. The optimal amounts of the probe and Cas12a-crRNA complex were 800 nM and 100 nM, respectively, and the optimal reaction temperature was 37 °C (Fig. 1E–H).

Based on the above experiments, we speculated that the sensitivity of one-pot assay could be improved by increasing the initial amplification rate of RPA and reducing the initial cis-activity of Cas12a. Then here we designed two crRNAs targeting the conserved region of SARS-CoV-2 N gene, one with canonical protospacer adjacent motif (cPAM: TTTV) and the other with suboptimal protospacer adjacent motif (sPAM). Two primer sets covering the crRNA targets were also designed, primer set 1 amplifying 262bp of N gene at loci 28841 to 29103 and primer set 2 amplifying 121bp of N gene at loci 28870 to 28990 (NCBI RefSeq: NC_045512.2) (Fig. 2A). Primer set 2 had a quicker and higher isothermal amplification than primer set 1, and the RPA replicon began to accumulate significantly about 5 min later with primer set 2, while 6 min later with primer set 1 (Fig. 2B S3E). On the other hand, the trans-activity of Cas12a/sPAM could be detected at 6 min, but at 4 min for Cas12a/cPAM (Fig. 2C, S3F). Then we created four one-pot assays by combining two primer sets with each crRNA. The quicker and higher amplification primer set 2 achieved a LOD of $10^{-17}$and $10^{-18}$ M at 40 min in one-pot assay with cPAM and sPAM respectively, nearly similar level with two-pot assay. By contrast, the lower amplification primer set 1 reached only $10^{-16}$ M at 40 min even with suboptimal PAM, and merely $10^{-11}$ M with canonical PAM (Fig. 2D–K). The results demonstrated that reliable and highly sensitive one-pot CORDSv2-SARS has been developed successfully. With the same principle of CORDSv2-SARS, ultrasensitive one-pot methods for multiple targets (CORDSv2-ASFV, CORDSv2-HPV16/18) have also been established quickly by screening highly efficient RPA primers and slow-pace crRNA rationally. LOD of CORDSv2-HPV16 and 18 could reach $10^{-16}$ and$10^{-17}$ M at 60 min respectively (Figs. S4A–G, S5A-G). The sensitivity for all the targets via CORDSv2 could reach up to, sometimes even higher than the level of the traditional two-pot assay.

### 2.2. Assessment of CORDSv2 on SARS-CoV-2 and ASFV detection

In order to detect SARS-CoV-2, the combination of primer set 2 and

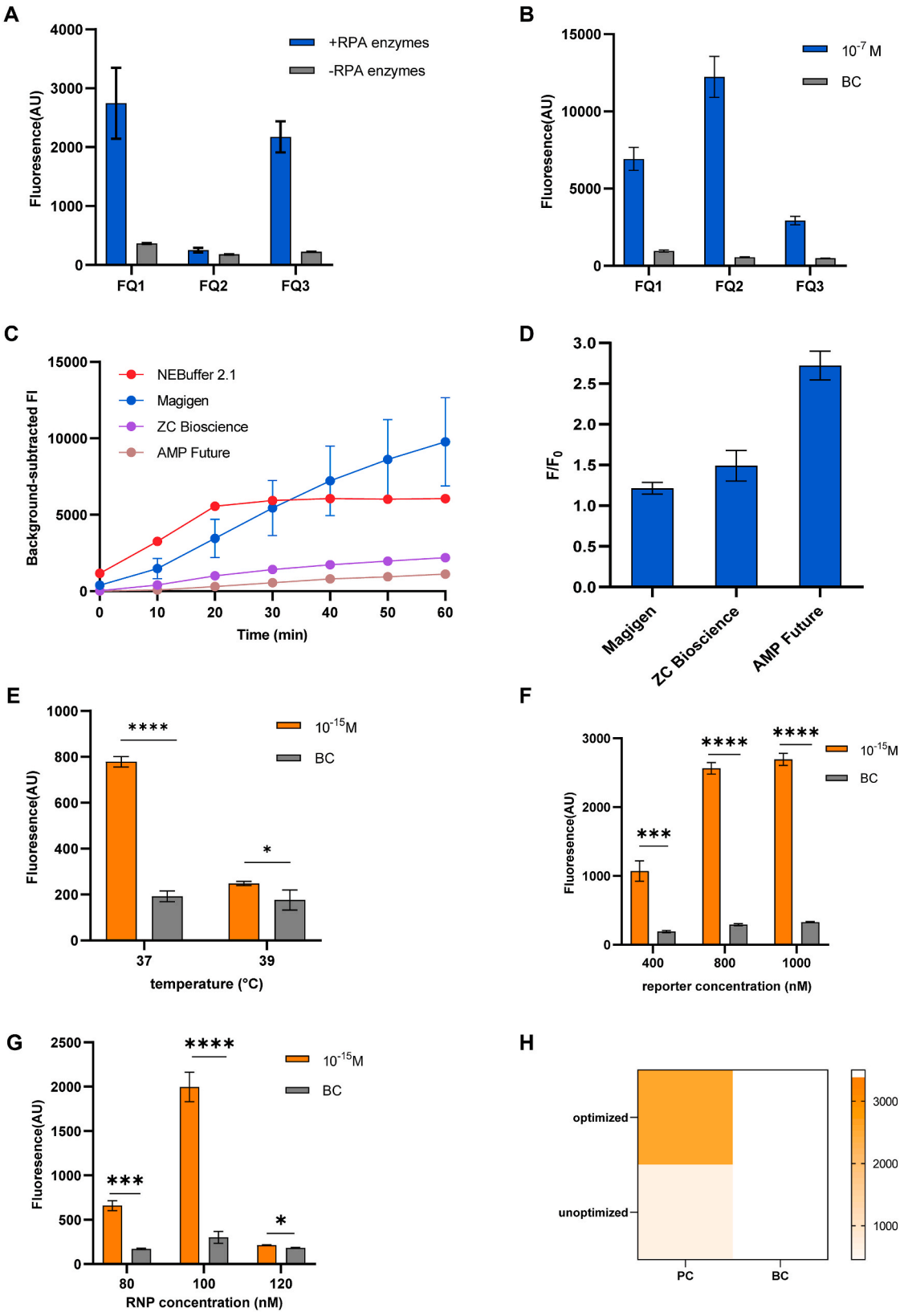
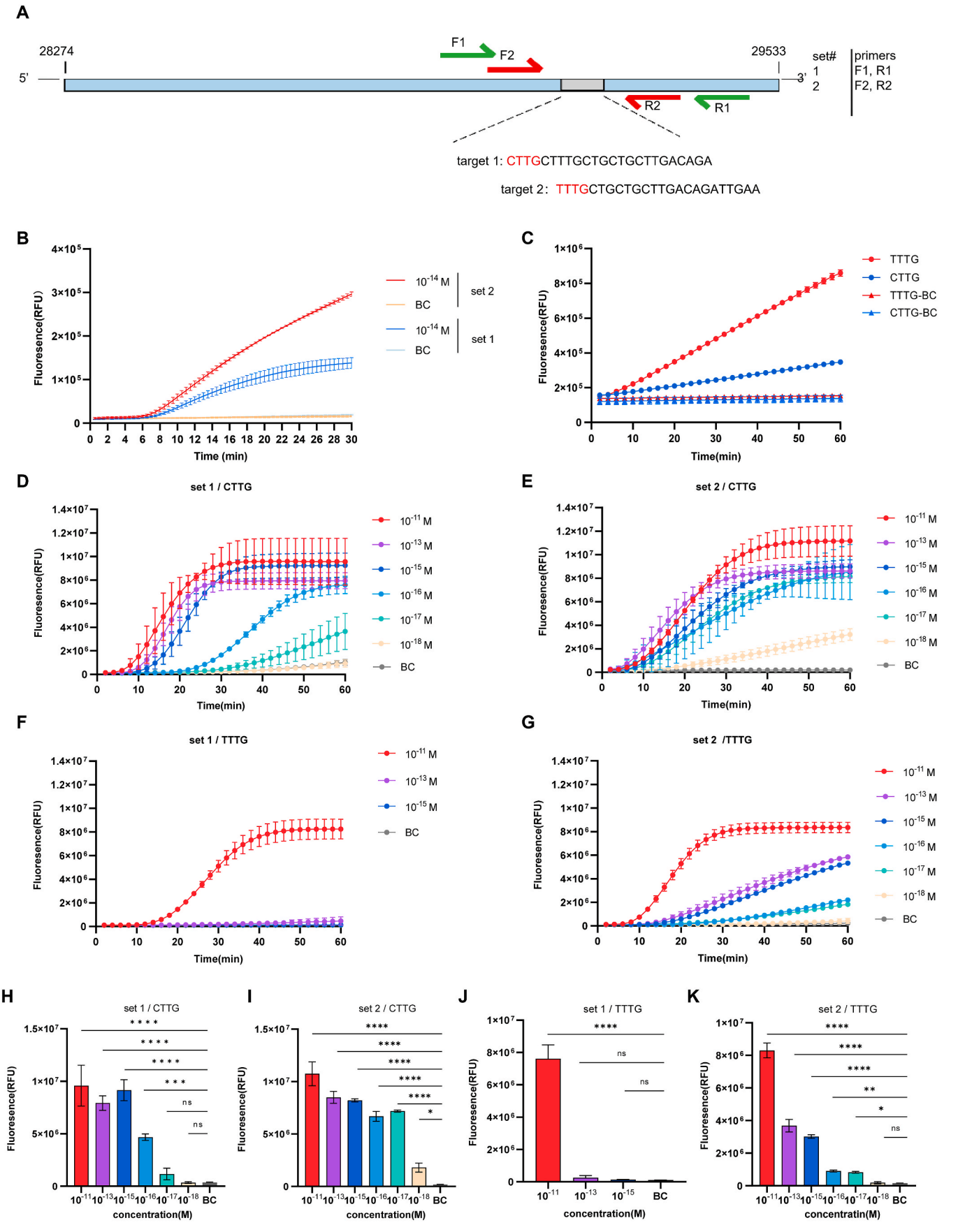



**Fig. 1.** Optimization of the one-pot system. (A) Stability analysis of three fluorescent probes in the RPA system at 30 min, -RPA enzyme: RPA system excluding amplification enzyme, +RPA enzyme: RPA system containing amplification enzyme. (B) Cleavage preference of LbCas12a for three fluorescent probes. (C) Collateral cleavage kinetics analysis of LbCas12a in NEBuffer 2.1 and buffer environment of three RPA kits. (D) Endpoint fluorescence ratio of Magigen-, ZC Bioscience- and AMP Future-based one-pot reaction at 1 h. F: fluorescence of one-pot reaction with DNA substrate. F0: fluorescence of one-pot reaction without DNA substrate. (E–G) Optimization of reaction temperature, probe concentration, RNP dose in the one-pot system. (H) Endpoint fluorescence comparison of the one-pot system before and after optimization at 1 h. In all graphs, error bars represent the means ± standard deviation (SD) of 3 replicates. PC: positive control with templates. BC: blank control without templates. Significance is considered at *p < 0.05, **p < 0.01, ***p < 0.001, ****p < 0.0001; ns indicates no significance.




*(caption on next page)*

**Fig. 2.** Comparative analysis of CORDSv2 reactions mediated by different primer sets associated with suboptimal PAM or canonical PAM. (A) Schematic representation of the SARS-CoV-2 N gene. The forward (F) and reverse (R) primers are represented by arrows. (B) Amplification kinetics of two primer sets targeting N gene with real-time fluorescent RPA, fluorescent signal was measured every 30 s. (C) Kinetics of CRISPR/Cas12a collateral cleavage mediated by suboptimal PAM (CTTG) and canonical PAM(TTTG) in N gene, the concentration of target substrates is $10^{-9}$ M. (D–G) Fluorescence kinetics of CORDSv2 reactions mediated by different primer sets associated with suboptimal PAM or canonical PAM at varying DNA input concentrations. (H–K) Limit of detection of CORDSv2 reactions mediated by different primer sets associated with suboptimal PAM or canonical PAM at 40 min. Set1/CTTG represents the CORDSv2 reaction mediated by primer set 1, suboptimal PAM(CTTG), and so on. In all graphs, error bars represent the means ± standard deviation(SD) of 3 replicates. BC: blank control without templates. Significance is considered at *p < 0.05, **p < 0.01, ***p < 0.001, ****p < 0.0001; ns indicates no significance.

sPAM crRNA (CUUUGCUGCUGCUUGACAGA) was selected, and 5 U M-MuLV reverse transcriptase and 0.05 U RNase H, were added to establish RT-CORDSv2 (Fig. S6). When using the pUC57-N plasmid as substrate, the detection limit of lateral flow strip was $10^{-15}$ M, inferior to fluorescence readout $10^{-18}$ M (Fig. 3B and C). We then applied RT-CORDSv2 to measure SARS-CoV-2 virus samples. Viral RNA was directly transferred into the RT-CORDSv2 tube and incubated at 37 °C for 40 min.18 samples with< 35 Ct value showed RT-CORDSv2 positive via fluorescence readout and lateral flow strip, and 6 samples with >35 Ct value showed RT-CORDSv2 negative via fluorescence readout and lateral flow strip (100% sensitivity and 100% specificity) (Fig. 3D–F, S7). The results indicated RT step was also efficient at 37 °C in RT-CORDSv2, more favorable than the higher temperature of 42 °C in sPAMC (Lu et al., 2022).

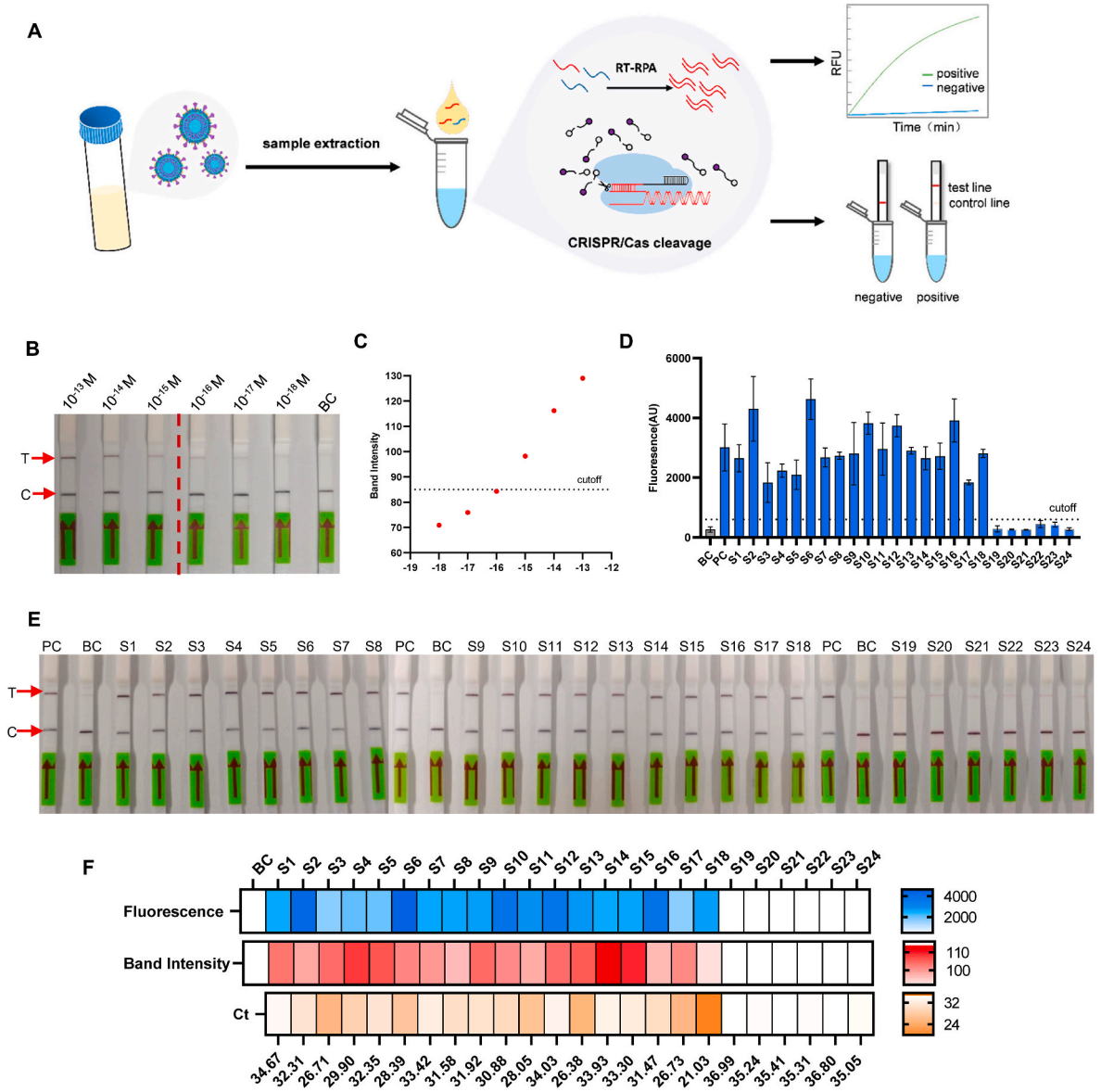



**Fig. 3.** Sensitive SARS-CoV-2 detection using RT-CORDSv2 system via fluorescence sensing or lateral flow test. (A) Schematic diagram of SARS- CoV-2 detection using RT-CORDSv2 system. (B) Limit of detection of SARS-CoV-2 using CORDSv2 system via lateral flow test after 40 min, using the pUC57-N plasmid as substrate. (C) The gray value of the test band at different target concentrations. (D) Virus sample detection of SARS-CoV-2 using RT-CORDSv2 system via fluorescence sensing. (E) Virus sample detection of SARS-CoV-2 using RT-CORDSv2 system via lateral flow strip. (F) Comparison of the virus sample detection using the RT-CORDSv2 system via fluorescence sensing, RT-CORDSv2 system via lateral flow strip, and RT-qPCR. In all graphs, error bars represent the means ± standard deviation(SD) of 3 replicates. PC: positive control with templates. BC: blank control without templates.

Furthermore, we also attempted to apply CORDSv2 for ASFV detection (Fig. 4A). After RPA primer and crRNA screening, the LOD of fluorescence CORDSv2 reached $10^{-18}$ M (Fig. 4B, S8). The LOD of lateral flow CORDSv2 reached $10^{-15}$ M by naked-eye observation and gray value analysis (Fig. 4C and D). To access the specificity of CORDSv2-ASFV, we tested 12 other porcine viruses simultaneously. And there was no cross-reaction with all 12 viruses, indicating high specificity for ASFV detection (Fig. 4E and F). Finally, a total of 15 swine serum samples were used to evaluate the performance of CORDSv2-ASFV on clinical samples. For samples with <35 Ct value, CORDSv2-ASFV with fluorescence readout had a sensitivity of 100% (9/9), but less sensitivity of 78% with lateral flow strip (7/9) (Fig. 4G–I, S9A, S9B). Compared with fluorescence readout, lateral flow strip assay has been demonstrated less sensitive by many research (Arizti-Sanz et al., 2022; Bai et al., 2019). Generally, Ct > 35 would represent very low viral titer and the sample with Ct > 35 would be considered as suspicious as well. So when using the CORDSv2 for ASFV and SARS-CoV-2, the suspicious samples with Ct > 35 might be tested as negative.

### 2.3. Portable CORDSv2 for POC diagnosis

We have developed the sensitive and specific CORDSv2 with simple handling. To facilitate its application towards POCT, we further designed a compact portable detection device hippo-CORDS (Heating and Imaging Powerfully Portable device for One-pot Cas12a-based On-site and Rapid Detection System). Unlike other imaging-only devices, both heating and imaging modules were integrated compactly into this portable device (Fig. 5A). After sample addition, the reaction tube of CORSv2 was transferred to the device, in which the temperature was set at 37 °C in advance. After 40 min incubation, turned on the LED blue light and observed the fluorescence of detection with the naked eyes or took photos by smartphone (Fig. S10). We first measured the sensitivity of CORDSv2 with this device by using various amounts of plasmid as substrate. For CORDSv2-SARS, the LOD reached $10^{-17}$ M by this device, 10-fold less sensitive than the fluorescence detection by plate ($10^{-18}$ M) and 100-fold more sensitive than the lateral flow strip ($10^{-15}$ M) (Fig. 5B, D). For CORDSv2-ASFV, detection limit by the portable device also reached $10^{-17}$ M (Fig. 5C, E). Then we proceeded to validate its performance on sample detection. Among the 24 SARS-CoV-2 virus samples referred, the detection results were consistent with the former test by fluorescence plater and lateral flow strip (Fig. 5F and G). For ASFV serum samples detection, it had 97% sensitivity (29/30) for samples with <35 Ct value, less than fluorescence plater (100%, 9/9), yet higher than lateral flow strip (78%, 7/9) (Fig. 5H and I). One-step pipetting combing with a low-cost device made it a favorable choice for POCT.

Moreover, it is optimal to lyophilize all CORDSv2 components, except the target, into a single tube for users' convenience. We chose the CORDSv2-ASFV for the lyophilization test and then validated its performance. All the components were lyophilized into one tube, then 25 μL extracted nucleic acid was added into the tube (Fig. 6A, S11). The lyophilized system effectively responded to a target of $10^{-15}$ M after storage at 4 °C for 7 days or after storage at room temperature for 5 days (Fig. 6B–J).

### 2.4. Rapid selection of crRNA and primer with AutoCORDSv2

For one-pot ASFV detection, 45 crRNAs and corresponding primers were obtained automatically by AutoCORDSv2 within 3 h after 188 ASFV genomic sequences input. And the crRNA within the top 4 and its primers also was identified to be efficient in ono-pot CORDSv2 detection. In addition, rapid design for HPV16 detection was further conducted with AutoCORDSv2. 63 crRNAs and corresponding primers were also selected automatically within 6 h even after 777 HPV16 genomic sequences input. The crRNA and its primer among the selection were demonstrated to be effective in one-pot CORDSv2 detection. Therefore, AutoCORDSv2 could be a reliable and automatical tool to select crRNA and primers for CORDSv2 assay simply.

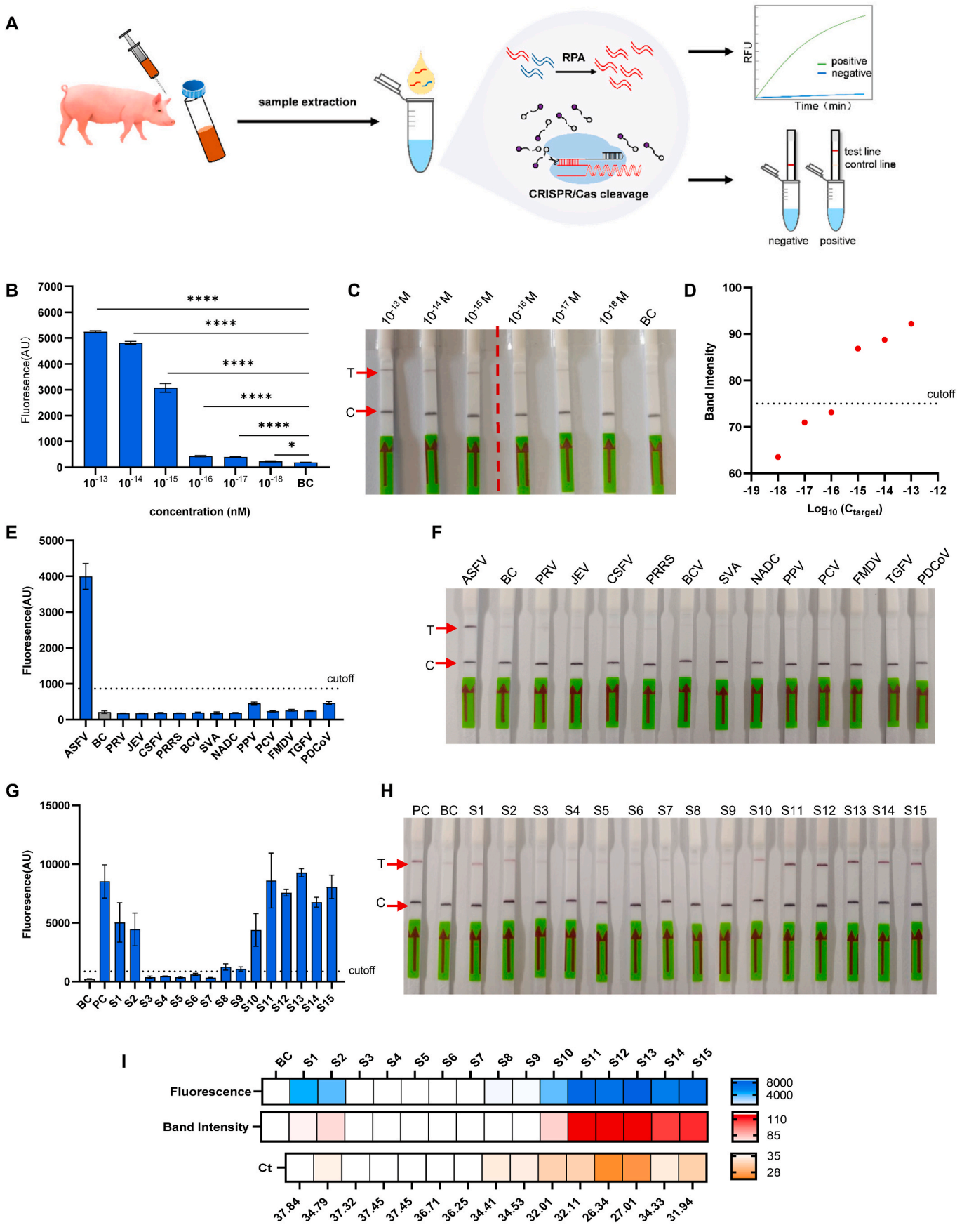
## 3. Discussion

One-pot RPA-CRISPR assays are gaining popularity in the CRISPR/Cas-based diagnostic field due to their simplicity. However, designing and optimizing these methods remains challenging and inefficient, primarily due to a lack of understanding of the underlying mechanisms. In our study, we introduced a rapid and rational strategy for developing the one-pot RPA-CRISPR method CORDSv2, which enabled sensitive and accurate detection of various targets, including SARS-CoV-2, ASFV, HPV16, and HPV18.

The main reason for the failure of one-pot RPA-CRISPR assays is the low amplification efficiency when CRISPR reagents are integrated into the isothermal amplification system, as active RNP can competitively bind and consume the replicons (Shao et al., 2023). Actually, $10^{-9}$ M templates are sufficient to activate CRISPR/Cas12a for clear distinguishment (Bai et al., 2019; He et al., 2022). The RPA amplicon usually could reach this level after a few minutes of amplification (Figs. S3A–D). Therefore, to achieve a sensitive one-pot RPA-CRISPR assay, it is necessary to artificially accelerate the RPA and/or slow down the CRISPR/Cas reaction, especially at the early stage. In our study, the sensitivity increased by 100-fold or even $10^6$-fold with a little faster RPA (with primer set 2). It could be one of the reasons that only a few two-pot primer sets also worked in the one-pot reaction (Aman et al., 2022). Here we found that faster RPA amplification within the first few minutes and the use of primers that amplify shorter DNA fragments contributed to improved sensitivity.

In addition to accelerating RPA, slightly slowing down the CRISPR/Cas reaction is another effective strategy for efficient one-pot RPA-CRISPR methods (Lin et al., 2023; Lu et al., 2022). It is well known that target binding is the rate-limiting step for Cas cleavage and PAM recognition happens firstly for target binding (Das et al., 2022; Strohkendl et al., 2018). For Cas12a, PAMs with TTTV could be favorable because PAM recognition domains prefer to bind the T at −4 to −2 position of PAM (Karvelis et al., 2020; Yamano et al., 2017). The suboptimal PAMs with one or two non-T at −4 to −2 position contributed to efficient one-pot RPA-CRISPR in sPAMC (Lu et al., 2022), yet all PAMs with one non-T at any position failed for one-pot ORCD method (Lin et al., 2023). Here our results indicated PAMs with one non-T at the −4 to −2 and T at −1 position worked well for one-pot method and our CORDSv2 method achieved a limit of detection (LOD) of 0.6 cp/μL for SARS-CoV-2 in 40 min, making it faster and more sensitive than other one-pot methods. Although Cas12a cleavage rate with our suboptimal PAMs was a little slower than canonical PAMs even just at the early stage of reaction, that was enough to make them perform much better when integrated with RPA in one-pot reaction. Almost equally sensitive detection can also be achieved for other targets, including ASFV and HPV16/18 via the similar one-pot CORDSv2 strategy. For ASFV serum sample detection with CORDSv2-ASFV, the detection sensitivity of Ct<35 samples was up to 97%. The high sensitivity of CORDSv2 for all four targets here suggested it could be suitable for more targets and viruses.

We also developed a compact, portable device called hippo-CORDS to make CORDSv2 more suitable for point-of-care testing (POCT). Hippo-CORDS integrated heating and imaging modules, making it more convenient for on-site testing and minimizing cross-contamination. With a LOD of 6 cp/μL, hippo-CORDS outperformed most other one-pot detection methods that use imaging-only devices (Aman et al., 2022; Lu et al., 2022). Its detection sensitivity and accuracy reached 100% for SARS-CoV-2 virus sample detection, surpassing many other one-pot detection methods with imaging devices (Aman et al., 2022; de Puig et al., 2021; Feng et al., 2021; Joung et al., 2020; Lu et al., 2022; Nguyen et al., 2022). However, the samples with Ct > 35 could be tested as negative by visual hippo-CORDS and the samples with Ct > 35 would be




*(caption on next page)*

**Fig. 4.** Sensitive and specific ASFV detection using CORDSv2 system via fluorescence sensing or lateral flow test. (A) Schematic diagram of ASFV detection using CORDSv2 system. (B) Limit of detection of ASFV using CORDSv2 system via fluorescence sensing after 60 min. (C) Limit of detection of ASFV using CORDSv2 system via lateral flow test after 60 min. (D) The gray value of the test band at different target concentrations. (E) Specificity of ASFV detection using CORDSv2 system via fluorescence sensing. (F) Specificity of ASFV detection using CORDSv2 system via lateral flow test. (G) Serum sample detection of ASFV using CORDSv2 system via fluorescence sensing. (H) Serum sample detection of ASFV using CORDSv2 system via lateral flow test. (I) Comparison of the serum sample detection using the CORDSv2 system via fluorescence sensing, CORDSv2 system via lateral flow strip, and qPCR. In all graphs, error bars represent the means ± standard deviation (SD) of 3 replicates. PC: positive control with templates. BC: blank control without templates. Significance is considered at *p < 0.05, **p < 0.01, ***p < 0.001, ****p < 0.0001; ns indicates no significance.

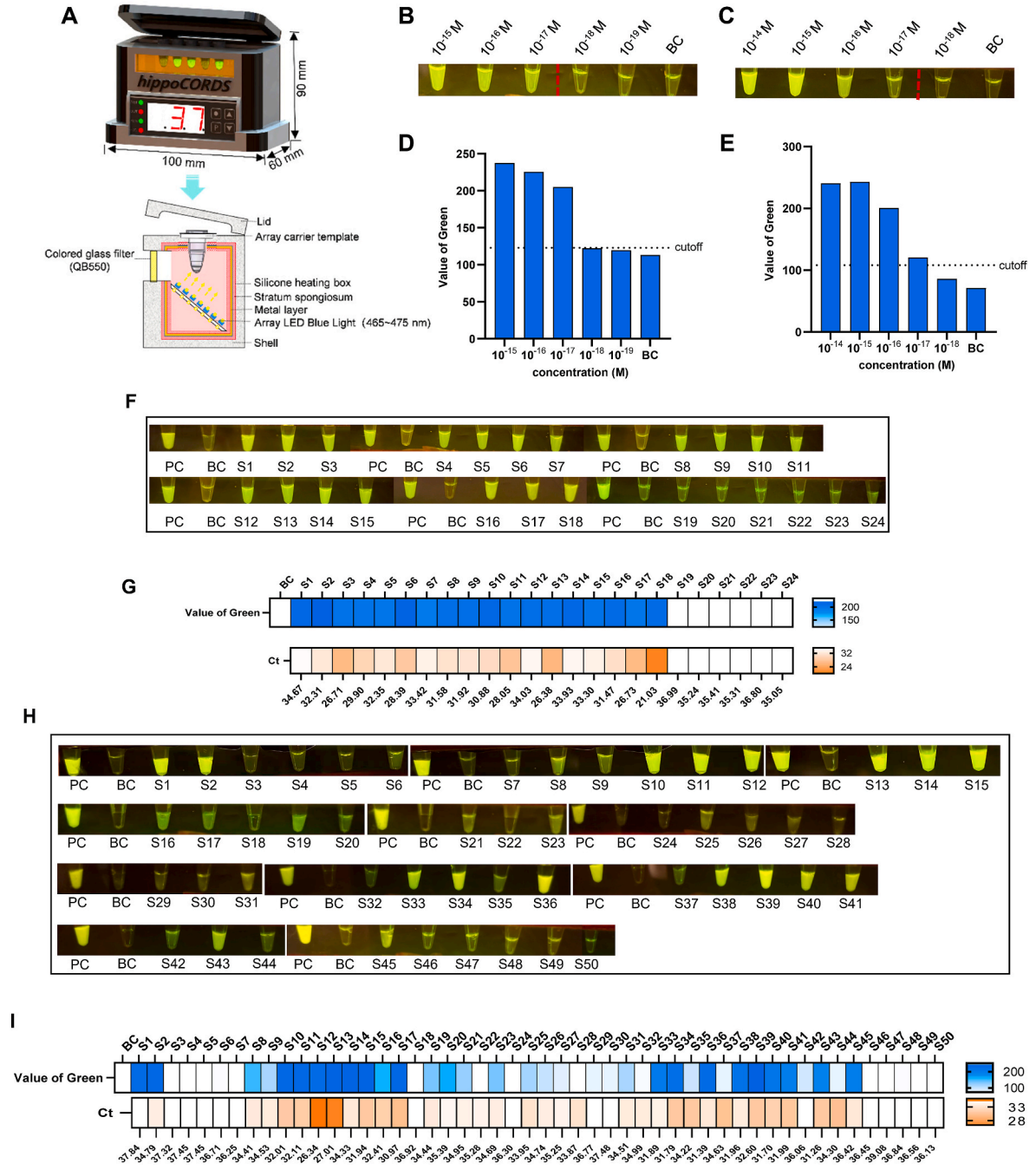



**Fig. 5.** Performance of the hippo-CORDS. (A) Construction of the hippo-CORDS. (B, D) Sensitivity of SARS-CoV-2 detection via the hippo-CORDS. (C, E) Sensitivity of ASFV detection via the hippo-CORDS. (F) Virus sample detection of SARS-CoV-2 via the hippo-CORDS. (G) Comparison of virus sample detection of SARS-CoV-2 via the hippo-CORDS and RT-qPCR. (H) Serum sample detection of ASFV via the hippo-CORDS. (I) Comparison of serum sample detection of ASFV via the hippo-CORDS and qPCR. All the reactions were incubated at 37 °C for 40–60 min. PC: positive control with templates. BC: blank control without templates.

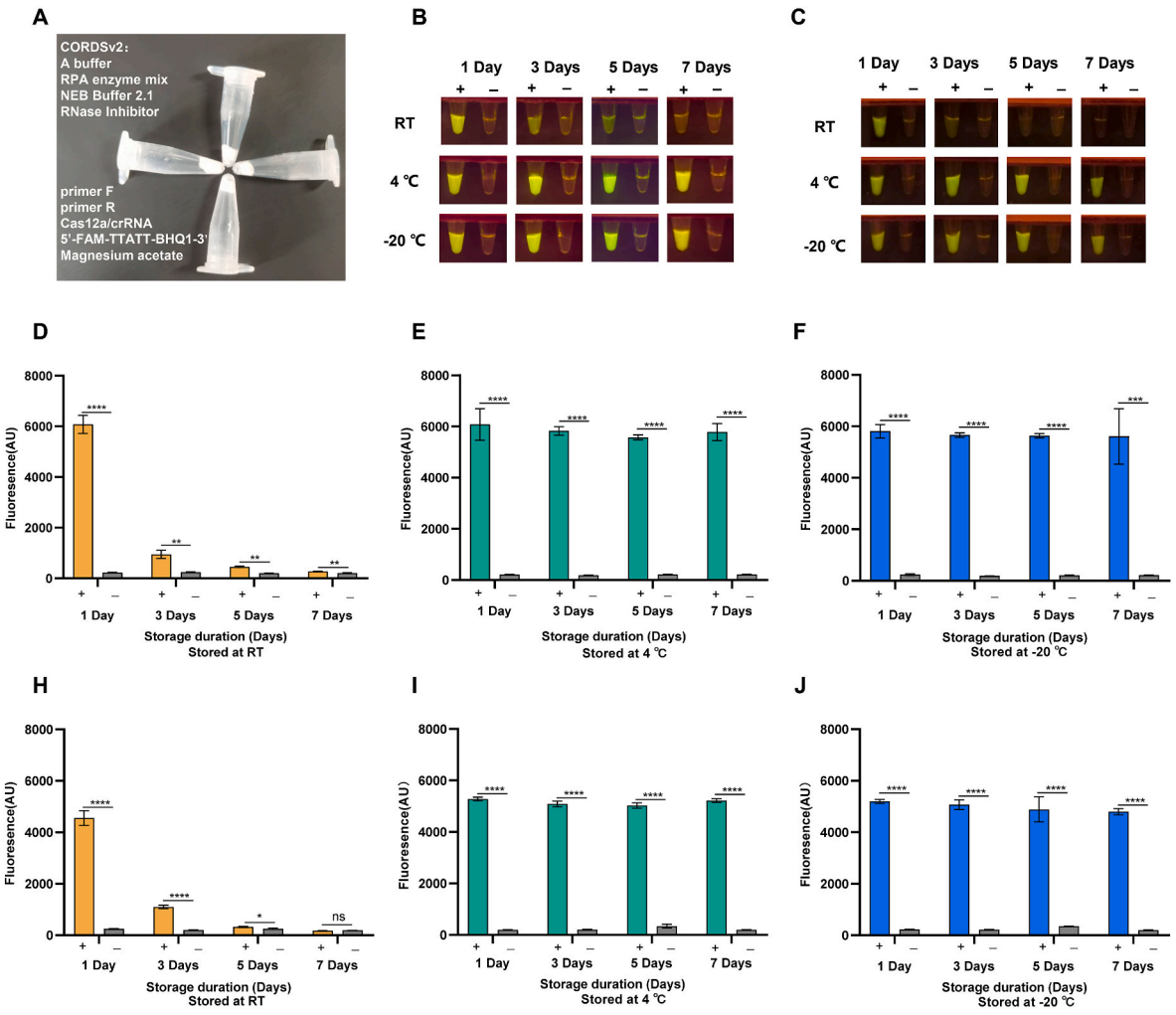



**Fig. 6.** Lyophilization of the CORDSv2 system. (A) Representation of lyophilized CORDSv2 reaction. (B) Stability of lyophilized CORDSv2 reaction via hippo-CORDS, using $10^{-13}$ M synthetic target as substrate. (C) Stability of lyophilized CORDSv2 reaction via hippo-CORDS, using $10^{-15}$ M synthetic target as substrate. (D–F) Stability of lyophilized CORDSv2 reaction via fluorescence sensing, using $10^{-13}$ M synthetic target as substrate. (G–H) Stability of lyophilized CORDSv2 reaction via fluorescence sensing, using $10^{-15}$ M synthetic target as substrate. +: one-pot assay with templates. -: one-pot assay without templates. All the reactions were incubated at 37 °C for 60 min. In all graphs, error bars represent the means ± standard deviation (SD) of 3 replicates. Significance is considered at *p < 0.05, **p < 0.01, ***p < 0.001, ****p < 0.0001; ns indicates no significance.

considered as suspicious by qPCR as well due to low viral titer.

## 4. Conclusions

By combining efficient one-pot lyophilization with the portable hippo-CORDS device, and the employment of automated design tools AutoCORDSv2, CORDSv2 represents a promising all-in-one CRISPR/Cas method for field testing. Our work contributes to advanced research in the field of rapid and accurate diagnosis in resource-limited settings. On the other hand, CORDSv2 also has several limitations, including the extraction of viral nucleic acids and nucleic acid amplification. Future work is needed to integrate the extraction of viral nucleic acid into CORDSv2, which might be solved by microfluidics (Chen et al., 2021; Nguyen et al., 2021; Ramachandran et al., 2020).

## Code availability

The AutoCORDSv2 software and the dataset used for validation are available at https://github.com/duao42/AutoCORDSv2.

## CRediT authorship contribution statement

**Cailing Lin:** designing and performing experiments, Formal analysis, Writing – original draft. **Feng Chen:** designing and performing experiments, constructing the imaging device, and, Writing – original draft. **Dongchao Huang:** bioinformatic, Formal analysis, of sequences, Writing – original draft. **Wenyan Li:** Formal analysis, Writing – original draft. **Changsheng He:** bioinformatic, Formal analysis, of sequences. **Yingjun Tang:** performing ASFV samples assay. **Xueping Li:** performing ASFV samples assay. **Can Liu:** performing SARS-CoV-2 samples assay. **Liya Han:** Investigation, data analysis. **Yunpeng Yang:** data analysis. **Yongchong Zhu:** Investigation. **Ruikang Chen:** Investigation. **Yuanju Shi:** advising on experimental design. **Chenglai Xia:** advising on experimental design. **Zhibin Yan:** advising on experimental design and experiment, Supervision. **Hongli Du:** Funding acquisition, conceiving and designing the study, experiment, Supervision. **Lizhen Huang:** Funding acquisition, conceiving and designing the study, experiment, Supervision, Writing – original draft, All authors reviewed and approved the manuscript.

## Declaration of competing interest

The authors declare that they have no known competing financial interests or personal relationships that could have appeared to influence the work reported in this paper.

## Data availability

Data availability and code availability are stated in the manuscript

## Acknowledgments

This work was supported by the National Natural Science Foundation of China, China [grant number 31871292]; Guangdong Basic and Applied Basic Research Foundation, China [grant number 2022A1515011733]; Science and Technology Program of Guangzhou, China [grant number 202206010073]; the CAS Key Laboratory of Regenerative Biology, Guangdong Provincial Key Laboratory of Stem Cell and Regenerative Medicine, Guangzhou Institutes of Biomedicine and Health, Chinese Academy of Sciences [grant number KLRB202103]; Science and Technology Program of Guangzhou, China [grant number 2023A03J0542]. We thank Professor Jun Li of the National University of Singapore for revising an earlier draft.

## Appendix A. Supplementary data

Supplementary data to this article can be found online at https://doi.org/10.1016/j.bios.2023.115609.

## References

Ackerman, C.M., Myhrvold, C., Thakku, S.G., Freije, C.A., Metsky, H.C., Yang, D.K., Ye, S. H., Boehm, C.K., Kosoko-Thoroddsen, T.F., Kehe, J., Nguyen, T.G., Carter, A., Kulesa, A., Barnes, J.R., Dugan, V.G., Hung, D.T., Blainey, P.C., Sabeti, P.C., 2020. Massively multiplexed nucleic acid detection with Cas13. Nature 582 (7811), 277–282.

Ali, Z., Aman, R., Mahas, A., Rao, G.S., Tehseen, M., Marsic, T., Salunke, R., Subudhi, A. K., Hala, S.M., Hamdan, S.M., Pain, A., Alofi, F.S., Alsomali, A., Hashem, A.M., Khogeer, A., Almontashiri, N.A.M., Abedalthagafi, M., Hassan, N., Mahfouz, M.M., 2020. iSCAN: an RT-LAMP-coupled CRISPR-Cas12 module for rapid, sensitive detection of SARS-CoV-2. Virus Res. 288, 198129.

Aman, R., Mahas, A., Marsic, T., Hassan, N., Mahfouz, M.M., 2020. Efficient, rapid, and sensitive detection of plant RNA viruses with one-pot RT-RPA-CRISPR/Cas12a assay. Front. Microbiol. 11, 610872.

Aman, R., Marsic, T., Sivakrishna Rao, G., Mahas, A., Ali, Z., Alsanea, M., Al-Qahtani, A., Alhamlan, F., Mahfouz, M., 2022. iSCAN-V2: a one-pot RT-RPA-CRISPR/cas12b assay for point-of-care SARS-CoV-2 detection. Front. Bioeng. Biotechnol. 9, 800104.

Arizti-Sanz, J., Bradley, A., Zhang, Y.B., Boehm, C.K., Freije, C.A., Grunberg, M.E., Kosoko-Thoroddsen, T.F., Welch, N.L., Pillai, P.P., Mantena, S., Kim, G., Uwanibe, J. N., John, O.G., Eromon, P.E., Kocher, G., Gross, R., Lee, J.S., Hensley, L.E., MacInnis, B.L., Johnson, J., Springer, M., Happi, C.T., Sabeti, P.C., Myhrvold, C., 2022. Simplified Cas13-based assays for the fast identification of SARS-CoV-2 and its variants. Nat. Biomed. Eng. 6 (8), 932–943.

Bai, J., Lin, H., Li, H., Zhou, Y., Liu, J., Zhong, G., Wu, L., Jiang, W., Du, H., Yang, J., Xie, Q., Huang, L., 2019. Cas12a-Based on-site and rapid nucleic acid detection of African swine fever. Front. Microbiol. 10, 2830.

Broughton, J.P., Deng, X., Yu, G., Fasching, C.L., Servellita, V., Singh, J., Miao, X., Streithorst, J.A., Granados, A., Sotomayor-Gonzalez, A., Zorn, K., Gopez, A., Hsu, E., Gu, W., Miller, S., Pan, C.Y., Guevara, H., Wadford, D.A., Chen, J.S., Chiu, C.Y., 2020. DETECTOR CRISPR-Cas12-based detection of SARS-CoV-2. Nat. Biotechnol. 38 (7), 870–874.

Chen, F.E., Lee, P.W., Trick, A.Y., Park, J.S., Chen, L., Shah, K., Mostafa, H., Carroll, K.C., Hsieh, K., Wang, T.H., 2021. Point-of-care CRISPR-Cas-assisted SARS-CoV-2 detection in an automated and portable droplet magnetofluidic device. Biosens. Bioelectron. 190, 113390.

Chen, Y., Xu, X., Wang, J., Zhang, Y., Zeng, W., Liu, Y., Zhang, X., 2022. Photoactivatable CRISPR/Cas12a strategy for one-pot DETECTR molecular. Anal. Chem. 94, 9724–9731.

Das, A., Goswami, H.N., Whyms, C.T., Sridhara, S., Li, H., 2022. Structural principles of CRISPR-Cas enzymes used in nucleic acid detection. J. Struct. Biol. 214 (1), 107838.

de Puig, H., Lee, R.A., Najjar, D., Tan, X., Soekensen, L.R., Angenent-Mari, N.M., Donghia, N.M., Weckman, N.E., Ory, A., Ng, C.F., Nguyen, P.Q., Mao, A.S., Ferrante, T.C., Lansberry, G., Sallum, H., Niemi, J., Collins, J.J., 2021. Minimally instrumented SHERLOCK (miSHERLOCK) for CRISPR-based point-of-care diagnosis of SARS-CoV-2 and emerging variants. Sci. Adv. 7, eabh2944.

Ding, X., Yin, K., Li, Z., Lalla, R.V., Ballesteros, E., Sfeir, M.M., Liu, C., 2020. Ultrasensitive and visual detection of SARS-CoV-2 using all-in-one dual CRISPR-Cas12a assay. Nat. Commun. 11 (1), 4711.

Feng, W., Peng, H., Xu, J., Liu, Y., Pabbaraju, K., Tipples, G., Joyce, M.A., Saffran, H.A., Tyrrell, D.L., Babiuk, S., Zhang, H., Le, X.C., 2021. Integrating reverse transcription recombinase polymerase amplification with CRISPR Technology for the one-tube assay of RNA. Anal. Chem. 93 (37), 12808–12816.

He, C., Lin, C., Mo, G., Xi, B., Li, A.A., Huang, D., Wan, Y., Chen, F., Liang, Y., Zuo, Q., Xu, W., Feng, D., Zhang, G., Han, L., Ke, C., Du, H., Huang, L., 2022. Rapid and accurate detection of SARS-CoV-2 mutations using a Cas12a-based sensing platform. Biosens. Bioelectron. 198, 113857.

Hu, M.L., Qiu, Z.Q., Bi, Z.R., Tian, T., Jiang, Y.Z., Zhou, X.M., 2022. Photocontrolled crRNA activation enables robust CRISPR-Cas12a diagnostics. In: Proceedings of the National Academy of Sciences of the United States of America, vol. 119, e2202034119, 26.

Joung, J., Ladha, A., Saito, M., Kim, N.G., Woolley, A.E., Segel, M., Barretto, R.P.J., Ranu, A., Macrae, R.K., Faure, G., Ioannidi, E.I., Krajeski, R.N., Bruneau, R., Huang, M.W., Yu, X.G., Li, J.Z., Walker, B.D., Hung, D.T., Greninger, A.L., Jerome, K. R., Gootenberg, J.S., Abudayyeh, O.O., Zhang, F., 2020. Detection of SARS-CoV-2 with SHERLOCK One-Pot Testing. N. Engl. J. Med. 383 (15), 1492–1494.

Karvelis, T., Bigelyte, G., Young, J.K., Hou, Z.L., Zedaveinyte, R., Budre, K., Paulraj, S., Djukanovic, V., Gasior, S., Silanskas, A., Venclovas, C., Siksnys, V., 2020. PAM recognition by miniature CRISPR-Cas12f nucleases triggers programmable double-stranded DNA target cleavage. Nucleic Acids Res. 48 (9), 5016–5023.

Kellner, M.J., Koob, J.G., Gootenberg, J.S., Abudayyeh, O.O., Zhang, F., 2019. SHERLOCK: nucleic acid detection with CRISPR nucleases. Nat. Protoc. 14 (10), 2986–3012.

Kostyusheva, A., Brezgin, S., Babin, Y., Vasilyeva, I., Glebe, D., Kostyushev, D., Chulanov, V., 2022. CRISPR-Cas systems for diagnosing infectious diseases. Methods 203, 431–446.

Lee, C.Y., Degani, I., Cheong, J., Lee, J.H., Choi, H.J., Cheon, J., Lee, H., 2021. Fluorescence polarization system for rapid COVID-19 diagnosis. Biosens. Bioelectron. 178, 113049.

Lee, R.A., Puig, H., Nguyen, P.Q., Angenent-Mari, N.M., Donghia, N.M., McGee, J.P., Dvorin, J.D., Klapperich, C.M., Pollock, N.R., Collins, J.J., 2020. Ultrasensitive CRISPR-based diagnostic for field-applicable detection of Plasmodium species in symptomatic and asymptomatic malaria. Proc. Natl. Acad. Sci. U. S. A. 117 (41), 25722–25731.

Li, X., Zheng, T., Gao, L., Li, F., Hou, X., Wu, P., 2020. Recombinase polymerase amplification : from principle to performance. Chemical Journal of Chinese Universities-Chinese 41 (12), 2587–2597.

Li, S.-Y., Cheng, Q.-X., Wang, J.-M., Li, X.-Y., Zhang, Z.-L., Gao, S., Cao, R.-B., Zhao, G.-P., Wang, J., 2018. CRISPR-Cas12a-assisted nucleic acid detection. Cell Discovery 4, 20.

Lin, K., Guo, J., Guo, X., Li, Q., Li, X., Sun, Z., Zhao, Z., Weng, J., Wu, J., Zhang, R., Li, B., 2023. Fast and visual detection of nucleic acids using a one-step RPA-CRISPR detection (ORCD) system unrestricted by the PAM. Anal. Chim. Acta 1248, 340938.

Lu, S., Tong, X., Han, Y., Zhang, K., Zhang, Y., Chen, Q., Duan, J., Lei, X., Huang, M., Qiu, Y., Zhang, D.Y., Zhou, X., Zhang, Y., Yin, H., 2022. Fast and sensitive detection of SARS-CoV-2 RNA using suboptimal protospacer adjacent motifs for Cas12a. Nat. Biomed. Eng. 6 (3), 286–297.

Malci, K., Walls, L.E., Rios-Solis, L., 2022. Rational design of CRISPR/Cas12a-RPA based one-pot COVID-19 detection with design of experiments. ACS Synth. Biol. 11 (4), 1555–1567.

Nguyen, L.T., Macaluso, N.C., Pizzano, B.L.M., Cash, M.N., Spacek, J., Karasek, J., Miller, M.R., Lednicky, J.A., Dinglasan, R.R., Salemi, M., Jain, P.K., 2022. A thermostable Cas12b from Brevibacillus leverages one-pot discrimination of SARS-CoV-2 variants of concern. EBioMedicine 77, 103926, 103926.

Nguyen, P.Q., Soenksen, L.R., Donghia, N.M., Angenent-Mari, N.M., de Puig, H., Huang, A., Lee, R., Slomovic, S., Galbersanini, T., Lansberry, G., Sallum, H.M., Zhao, E.M., Niemi, J.B., Collins, J.J., 2021. Wearable materials with embedded synthetic biology sensors for biomolecule detection. Nat. Biotechnol. 39 (11), 1366–1374.

Ramachandran, A., Huyke, D.A., Sharma, E., Sahoo, M.K., Huang, C., Banaei, N., Pinsky, B.A., Santiago, J.G., 2020. Electric field-driven microfluidics for rapid CRISPR-based diagnostics and its application to detection of SARS-CoV-2. In: Proceedings of the National Academy of Sciences of the United States of America, vol. 117, pp. 29518–29525, 47.

Shao, F., Park, J.S., Zhao, G., Hsieh, K., Wang, T.H., 2023. Elucidating the role of CRISPR/Cas in single-step isothermal nucleic acid amplification testing assays. Anal. Chem. 95 (7), 3873–3882.

Strohkendl, I., Saifuddin, F.A., Rybarski, J.R., Finkelstein, I.J., Russell, R., 2018. Kinetic basis for DNA target specificity of CRISPRCas12a. Mol. Cell 71 (5), 816–824 e813.

Teng, F., Guo, L., Cui, T., Wang, X.G., Xu, K., Gao, Q., Zhou, Q., Li, W., 2019. CDetection: CRISPR-Cas12b-based DNA detection with sub-attomolar sensitivity and single-base specificity. Genome Biol. 20 (1), 132.

Wu, X., Tay, J.K., Goh, C.K., Chan, C., Lee, Y.H., Springs, S.L., Wang, Y., Loh, K.S., Lu, T. K., Yu, H., 2021. Digital CRISPR-based method for the rapid detection and absolute quantification of nucleic acids. Biomaterials 274, 120876.

Xia, L., Yin, J., Zhuang, J., Yin, W., Zou, Z., Mu, Y., 2023. Adsorption-free self-priming direct digital dual-crRNA CRISPR/Cas12a-Assisted chip for ultrasensitive detection of pathogens. Anal. Chem. 95 (10), 4744–4752.

Yamano, T., Zetsche, B., Ishitani, R., Zhang, F., Nishimasu, H., Nureki, O., 2017. Structural basis for the canonical and non-canonical PAM recognition by CRISPR-cpf1. Mol. Cell 67 (4), 633–645 .e3.

Zhang, L., Jiang, H., Zhu, Z., Liu, J., Li, B., 2022. Integrating CRISPR/Cas within Isothermal Amplification for Point-Of-Care Assay of Nucleic Acid, vol. 243. Talanta.

Zyrina, N.V., Antipova, V.N., 2021. Nonspecific synthesis in the reactions of isothermal nucleic acid amplification. Biochemistry-Moscow 86 (7), 887–897.